THE JOURNAL OF PHYSICAL CHEMISTRY B

ARTICLE

pubs.acs.org/JPCB

Pore Shape of Honeycomb-Patterned Films: Modulation and Interfacial Behavior

Ling-Shu Wan,* Bei-Bei Ke, Jing Zhang, and Zhi-Kang Xu

MOE Key Laboratory of Macromolecular Synthesis and Functionalization, Department of Polymer Science and Engineering, Zhejiang University, Hangzhou 310027, China

Supporting Information

ABSTRACT: The control of the pore size of honeycomb-patterned films has been more or less involved in most work on the topic of breath figures. Modulation of the pore shape was largely ignored, although it is important to applications in replica molding, filtration, particle assembly, and cell culture. This article reports a tunable pore shape for patterned films prepared from commercially available polystyrene (PS). We investigated the effects of solvents including tetrahydrofuran (THF) and chloroform (CF) and hydrophilic additives including poly(*N*,*N*-dimethylaminoethyl methacrylate) (PDMAEMA), poly(ethylene glycol) (PEG), and poly(*N*-vinyl pyrrolidone) (PVP). Water droplets on/in the polymer solutions were observed and analyzed for simulating the formation and stabilization of breath figures. Interfacial tensions of the studied systems were measured and considered as a main factor to modulate the pore shape. Results indicate that the pores gradually change from near-spherical to ellipsoidal with the increase of additive content when using CF as the solvent; however, only ellipsoidal pores are formed from the THF solution. It is demonstrated that the aggregation of the additives at the water/polymer solution interface is more efficient in the THF solution than that in the CF solution. This aggregation decreases the interfacial tension, stabilizes the condensed water droplets, and shapes the pores of the films. The results may facilitate our understanding of the dynamic breath figure process and provide a new pathway to prepare patterned films with different pore structures.

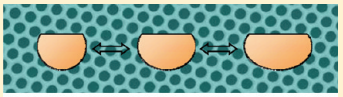

INTRODUCTION

The breath figure method, inspired by the foggy arrays of water droplets condensed on cool surfaces, has received increasing attention because it provides the facility to prepare patterned porous films.[1−3] These patterned films show great potential as functional materials such as optical and electronic devices,[4] energy storage,[5] catalyst supports,[6] templates,[7] cell culture scalfolds,[8] and superhydrophobic surfaces.[9] It is generally accepted that this method contains three steps as follows: (i) a polymer solution that contains highly volatile solvent is placed under a humidity environment, and water droplets nucleate and subsequently grow at the air/solution interface as the evaporative cooling; (ii) the polymer aggregates/deposits at the interfaces between the solution and the water droplets, creating a polymer envelope to prevent coalescence of the water droplets, which self-organize into a hexagonally ordered array by the Marangoni convection; (iii) with further evaporation of the solvent and the water droplets, film hardening occurs and a honeycomb-patterned porous structure is obtained.[1−3]

Up to now, the breath figure method has been applied to a variety of polymers such as star and comb-like polystyrenes,[10,11] polyimides,[12,13] polyion complexes,[14] and organometallic polymers.[15] Star polymers and amphiphilic block copolymers are generally believed to be good candidates, but their synthesis is quite complex and time-consuming.[16] It was reported that polystyrene (PS), a commercially available polymer without any polar groups, could also be fabricated into regular porous films. However, the process is much less robust, and the casting condition needs to be optimized.[17] As a result, surfactants or hydrophilic polymers were added to the casting solution to improve the film formation and to enhance the toleration of a wide range of casting conditions.[18−20] Undoubtedly, use of commercially available polymers can greatly facilitate the practical application of the breath figure method, but it is very important to understand the roles of the additives on the formation of breath figures and, then, to modulate the film structures including pore size and pore shape.

The modulation of pore size has been more or less involved in most work on the topic of breath figures. For example, the pore diameter can be controlled in the range of a few hundreds of nanometers to tens of micrometers by varying polymer structures or casting conditions such as polymer concentration and environment humidity.[21−24] Hierarchically ordered structures with multiscale sizes were achieved by directly casting the polymer solution on nonflat surfaces or by postphotopatterning.[25−28]

The pore shape is quite important to applications in replica molding, particle assembly, cell culture, and sensing.[24,29−31] Spherical and hemispherical microlens were prepared using the original honeycomb-patterned film and the peeled film as molding templates, respectively.[30] It was found that the hemispherical microlens had better projection properties than the spherical ones. Besides, hexagonally arranged circular pores can be transformed into different shapes (square, rectangular, or triangular) by mechanical stretching or shrinking.[29,32] However, the above-mentioned strategies for different pore shapes depend on secondary

Received: August 23, 2011
Revised: November 6, 2011
Published: December 12, 2011

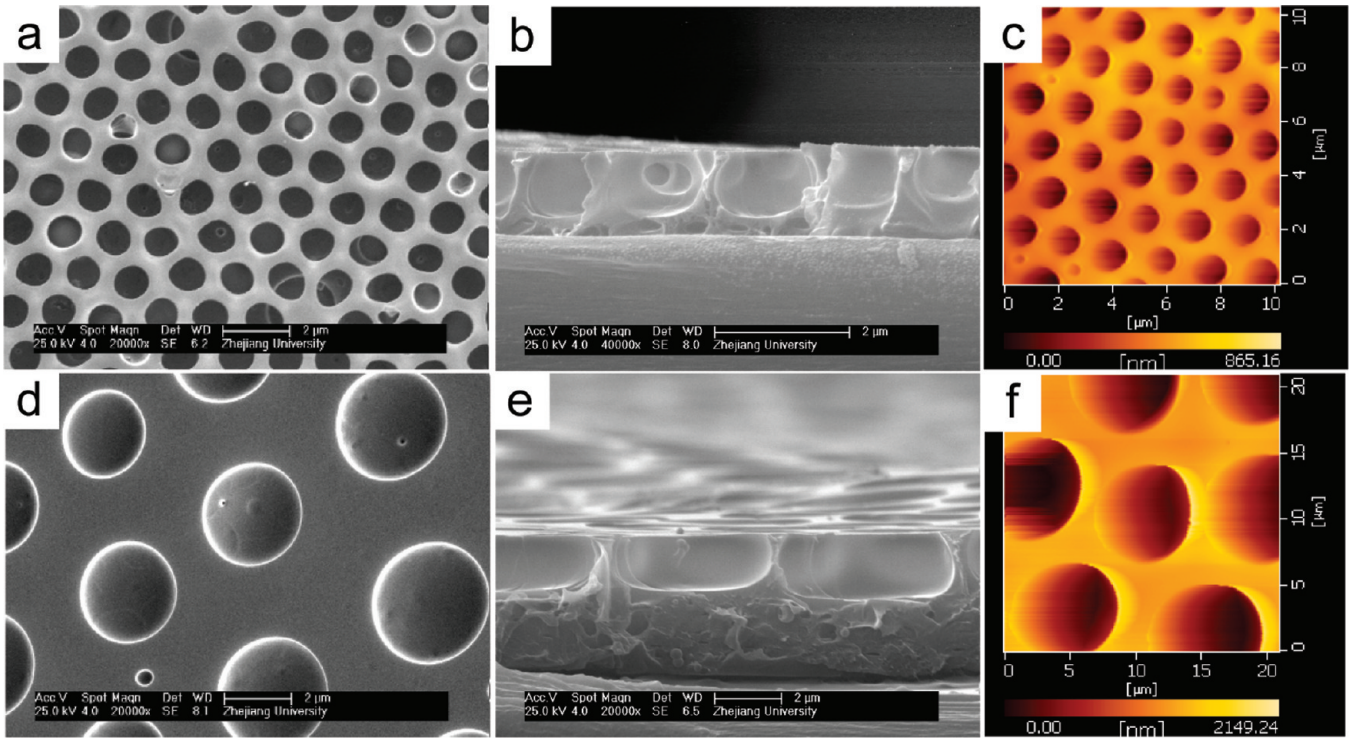

Figure 1. Micrographs of PS/PDMAEMA films using CF (a,b,c) or THF (d,e,f) as the solvent. (a,d) Top view and (b,e) cross-section of SEM images; (c,f) AFM height images. The concentrations of PS/PDMAEMA are 20/4 mg/mL.

processing. Direct preparation of honeycomb-patterned films with nonspherical pores has been scarcely reported. Differing from the commercially available PS, Qiao and his co-workers[33] first fabricated honeycomb-patterned films with a cylindrical pore structure from star polymers having a perfluoroalkyl end functional group. A difference in the pore shape was ascribed to the chain-end chemistry of the star polymers. Further investigation is required to conclude the rules governing the pore shape and its modulation.

In the present study, honeycomb-patterned films with different pore shapes were fabricated from commercially available PS by the breath figure method in which some water-soluble polymers such as poly(*N*,*N*-dimethylaminoethyl methacrylate), poly(*N*-vinyl pyrrolidone), and poly(ethylene glycol) were used as additives. Detailed study on the formation of these pore structures provides insights into the breath figure process and advances our knowledge in controlled development of films with various pore shapes.

EXPERIMENTAL SECTION

Materials. Polystyrene (PS, M_w = 235 000 g/mol, MWD = 2.89) was provided by Zhenjiang Chiemei Chemicals. Poly(*N*,*N*-dimethylaminoethyl methacrylate) (PDMAEMA, M_n = 11 300 g/mol, MWD = 1.51) was synthesized by ATRP using a reported procedure in tetrahydrofuran (THF).[11,34] Poly(ethylene glycol) (PEG, M_w = 10 000 g/mol) and poly(*N*-vinyl pyrrolidone) (PVP, K30) were obtained from Sinopharm Chemical Reagent Co. (China). Fluorescein sodium salt (99%, Sigma) and *p*-xylylene dichloride (XDC, 98%, Alfa Aesar) were used as received. Poly(ethylene terephthalate) (PET) film was kindly provided by Hangzhou Tape Factory and cleaned with acetone for 2 h before use. Water used in all experiments was deionized and ultrafiltrated to 18.2 MΩ with an ELGA LabWater system. All other reagents were analytical grade and used without further purification.

Preparation of Honeycomb-Patterned Films. The films were cast by the breath figure method according to the following procedure. PS and the additive (PDMAEMA, PEG, or PVP) were blended at different weight ratios and dissolved in chloroform (CF) or tetrahydrofuran (THF). An aliquot of 100 μL for each polymer solution was drop cast onto a PET substrate placed under a 2 L/min humid airflow. The humidity of the airflow was maintained to be above 70% by bubbling through deionized water and was measured by a hygro-thermograph (DT-321S, CEM Corporation). After solidification, the film was dried at room temperature.

Observation of Water Droplets in the Polymer Solutions. Deionized water was stained by a water-soluble red dye (0.01 mg/mL, Reactive red X-3b, Shanghai Chemical Reagent Co., China) and vertically dropped to the polymer solutions. The shape of the millimeter-scale water droplets was recorded by a digital camera and analyzed using ImageJ (version 1.42q by Wayne Rasband).

Adsorption of Fluorescein Sodium Salt. The PS/PDMAEMA film was immersed in XDC/*n*-heptane solution (1% w/v) at room temperature for quaternization and cross-linking.[34] After quaternization, a piece of film (2 × 4 cm^2) was immersed in 10 mL of fluorescein sodium salt aqueous solution (0.1 mg/mL, pH 7.0) and incubated at 25 °C for 24 h. Then, the films were washed with deionized water for six times. After being dried under reduced pressure at room temperature, fluorescence images of the fluorescein-adsorbed films were recorded by a confocal laser scanning microscopy.

Characterization. A field emission scanning electron microscope (FESEM, Sirion-100, FEI, USA) was used to observe the surface morphology of films after being sputtered with gold using

dx.doi.org/10.1021/jp208115u |*J. Phys. Chem. B* 2012, 116, 40–47

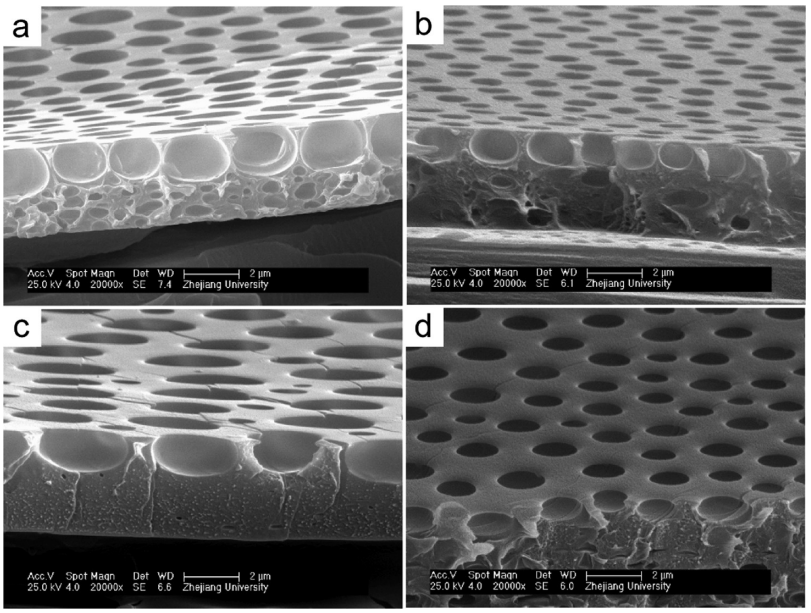

Figure 2. Cross-section micrographs of honeycomb-patterned films. (a) PS/PEG/CF; (b) PS/PVP/CF; (c) PS/PEG/THF; (d) PS/PVP/THF. The concentrations of PS/PEG and PS/PVP are 20/4 mg/mL.

ion sputter JFC-1100. Height images were recorded by atomic force microscopy (AFM, SEIKO SPI3800N) under tapping conditions. Confocal laser scanning microscopy (CLSM) was performed on a Leica TCS SP5 confocal setup mounted on a Leica DMI 6000 CS inverted microscope (Leica Microsystems, Wetzlar, Germany) and was operated under the Leica Application Suite Advanced Fluorescence (LAS AF) program. The surface tension of each polymer solution and interfacial tension between water and the polymer solution were measured on a DropMeter A-200 contact angle system (MAIST Vision Inspection & Measurement Ltd. Co., China) using the pendant drop technique.[35]

RESULTS

Effects of Solvents on Pore Shape. The breath figure method often uses organic solvents with high saturation vapor pressure, such as carbon disulfide (CS_2), CF, and THF, in which THF is miscible with water, whereas CS_2 and CF are not. In this work, CF and THF are chosen as solvents for the blends of PS and additives, and their effects on the pore shape were investigated. Figure 1 shows SEM and AFM images of the prepared films. Casting conditions such as solution concentration, relative humidity, and airflow speed were optimized (see the Supporting Information), and the weight ratio of PS and PDMAEMA was set as 5/1. When cast from CF solution, the film has an average pore diameter of about 1 μm. The pore shape in cross-section is near-spherical (Figure 1b). However, the film fabricated from THF solution has a larger pore diameter of about 3 μm, and the pore shape becomes ellipsoidal (Figure 1e).

It is clear that the solvents have a remarkable impact on the pore shape of the films. PS/PDMAEMA films with near-spherical and ellipsoidal pores were obtained from CF and THF solutions, respectively. Results of other polymer blends (PS/PEG and PS/PVP) provide further confirmation of the effects of solvents on the pore structures. Figure 2 shows the cross-section images of films prepared from PS/PEG and PS/PVP using different solvents. Obviously, PS/PEG and PS/PVP films have similar structures with those prepared from PS/PDMAEMA. CF solution results in pores with near-spherical shape (Figure 2a,b), whereas THF solution leads to ellipsoidal pores (Figure 2c,d). To quantitatively describe the pore shape, we define a pore shape factor R, which is equal to the ratio of the length of the minor axis (a) to the long axis (b) of the cross-section of the pore ($R = a/b$, Scheme 1). As estimated from the SEM images shown in Figures 1 and 2, R values of films prepared from CF solutions range from 0.75 to 0.78, whereas they fluctuate from 0.51 to 0.56 for those prepared from THF solutions. Besides, films prepared using CF as the solvent are generally more regular than that prepared from THF solution. The porous film made from PS/PEG/CF is multilayered, while that from PS/PEG/THF is single layered. These structures depend on the density of used solvents[36] and the interfacial tension.[37]

Scheme 1. Schematic Illustration of the Shape Factor R

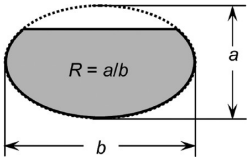

Effects of Additive Contents on Pore Shape. Figure 3 shows the SEM micrographs of films cast from CF solutions with different contents of PDMAEMA. Honeycomb-patterned films can be obtained from PS solution without any additives (Figure 3a). The pores are near-spherical with an R value of 0.92, which is very close to 1.0. With the increase of PDMAEMA content from 0 to 4, 7, and 10 mg/mL, the pores gradually change from near-spherical to ellipsoidal, and the R values decrease from 0.92 to 0.78, 0.72, and 0.69, respectively. Further increasing the concentration of PDMAEMA leads to irregular films.

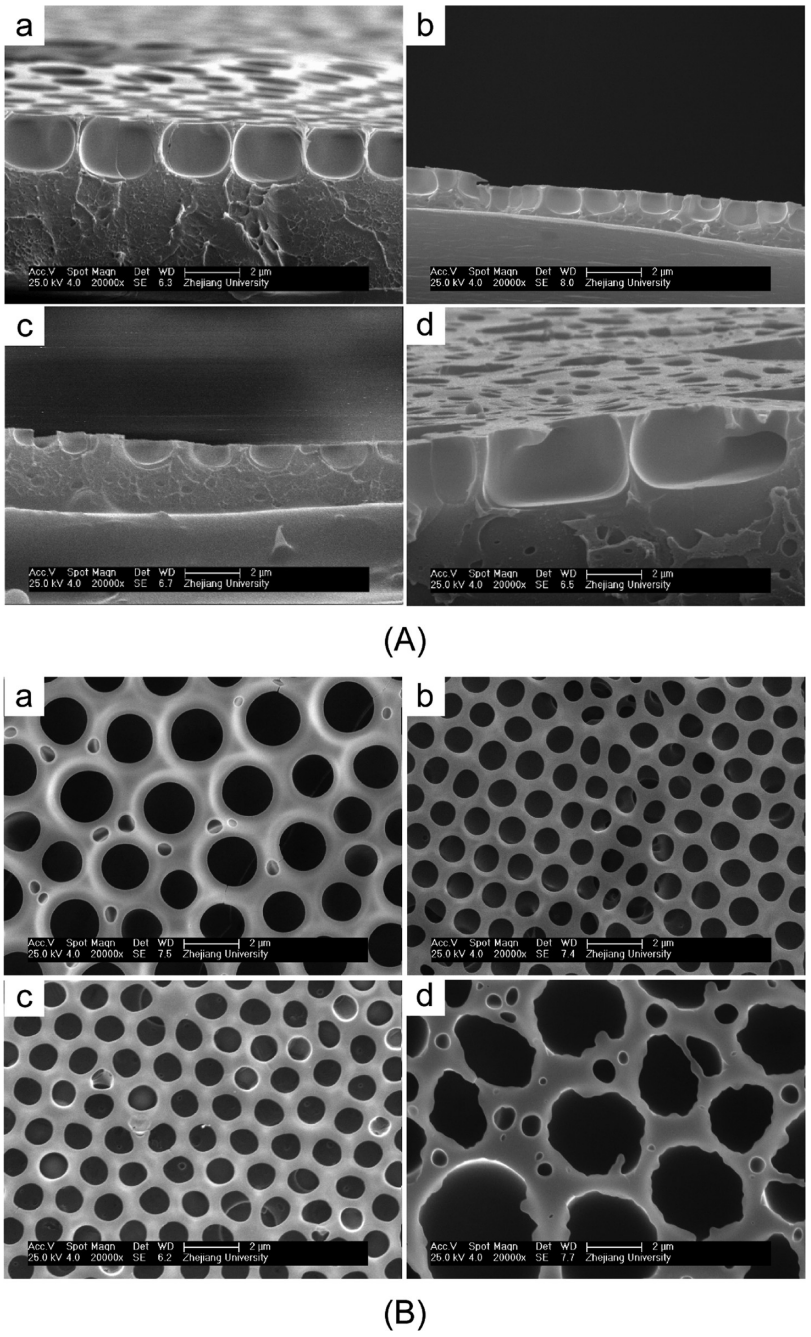

Figure 3. SEM images of films prepared with different PDMAEMA concentrations: (a) 0 mg/mL; (b) 4 mg/mL; (c) 7 mg/mL; (d) 10 mg/mL. The concentration of PS is 20 mg/mL, and the solvent is CF. (A) Cross-section. (B) Top surface.

However, the content of additives has a different influence on the pore shape of films fabricated from THF solutions (Figure 4). When THF solution of PS was employed in the breath figure method, patterned porous film cannot be formed. In contrast to the PS system, PS/PDMAEMA blend system is able to form patterned films with ellipsoidal pores. There is no obvious change in the pore shape when increasing the content of PDMAEMA in THF solution, and the *R* values are between 0.50 and 0.53.

Simulation of Water Droplets in the Polymer Solutions. In the breath figure process, the condensed water droplets act as dynamic templates and shape the pores. It is difficult to directly observe the condensed water droplets to determine the shape. Therefore, deionized water was directly dropped into the polymer solutions by microsyringe, and the millimeter-scale water droplets were observed to simulate the condensed water droplets in the breath figure process. Considering that the polymer solution was concentrated during the breath figure process,[2] effects of PS concentration on the shape of water droplets were first studied by keeping the ratio of PS to PDMAEMA constant. Figure 5 shows side views of the water droplets in PS/PDMAEMA solutions with different concentrations up to 100/20 mg/mL. Higher concentration is not achievable because of the solubility limit of PDMAEMA. The water droplets float on the CF solutions (Figure 5A), and the shape does not change with the

dx.doi.org/10.1021/jp208115u |*J. Phys. Chem. B* 2012, 116, 40–47

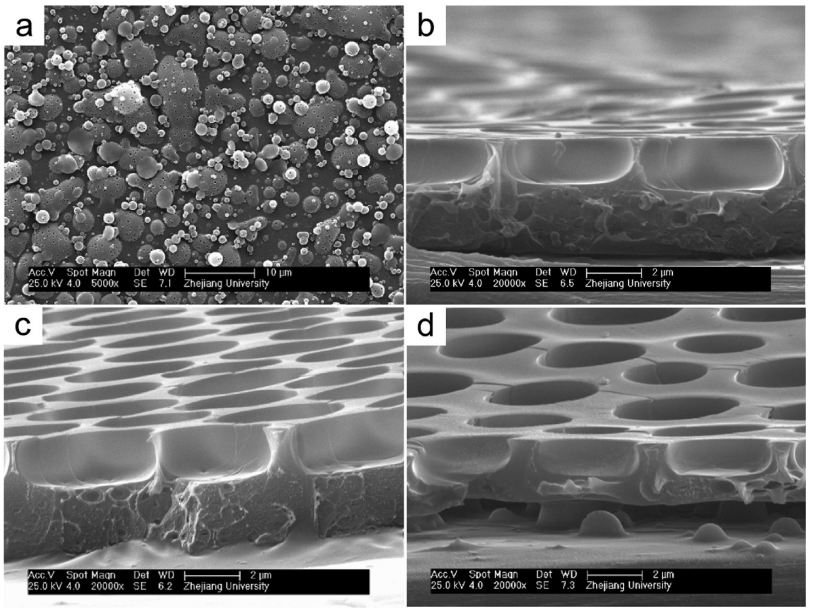

Figure 4. SEM images of films prepared with different PDMAEMA concentrations: (a) 0 mg/mL; (b) 4 mg/mL; (c) 7 mg/mL; (d) 10 mg/mL. The concentration of PS is 20 mg/mL, and the solvent is THF.

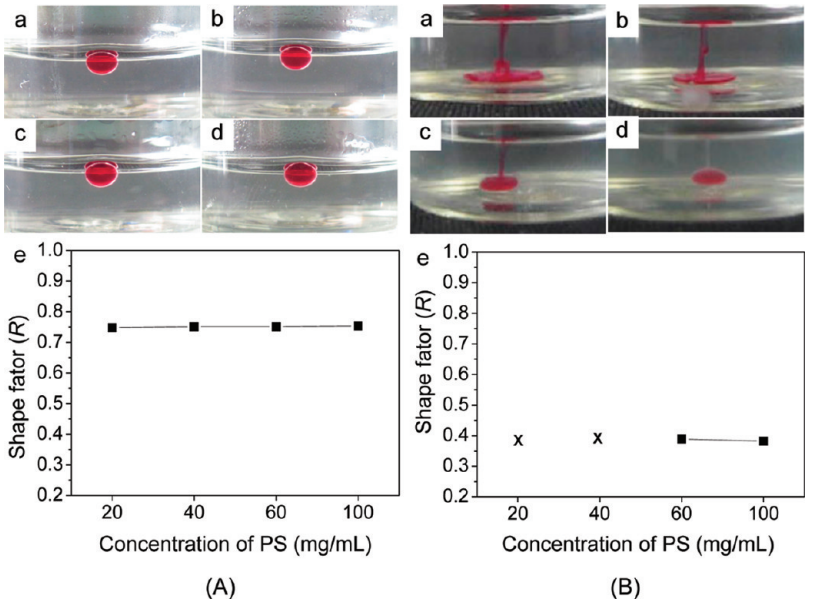

Figure 5. Simulated water droplets in solutions with different PS concentrations: (a) 20 mg/mL; (b) 40 mg/mL, (c) 60 mg/mL; (d) 100 mg/mL. The weight ratio of PS to PDMAEMA is kept constant at 5/1. (e) Dependence of shape factor *R* on the concentration of PS. Solvent: (A) CF and (B) THF.

concentration of PS/PDMAEMA. The *R* value is constant about 0.75. However, the appearance of the water droplets is different in the THF solutions. Since the density of water is larger than that of THF, they sink into the THF solutions (Figure 5B). The water droplets can be observed only in solutions with high concentration of 60/12 or 100/20 mg/mL, showing a shape factor *R* of about 0.40.

Influence of additive content was then investigated in solutions with a PS concentration of 100 mg/mL. For the CF solutions (Figure 6A), the shape of the water droplets changes from near-spherical to ellipsoidal with the increase of PDMAEMA content, and accordingly, the *R* values decrease from 0.88 to 0.75, 0.71, and 0.66. The simulated results are well consistent with those of the corresponding films. Water droplets in the THF solutions are different from those in the CF solutions (Figure 6B). Water mixes with the THF solution, and the PS cannot effectively stabilize the condensed water droplets if without hydrophilic additives. In PS/PDMAEMA solutions, the shape of the water droplets is ellipsoidal, and the *R* values are between 0.32 and 0.37, which almost keeps constant. This result is also in accordance with that of the corresponding films. Similar trends were observed in the solutions of PS/PEG and PS/PVP.

Interfacial Tensions between Water and the Polymer Solutions. The surface tensions of the solutions were measured

dx.doi.org/10.1021/jp208115u |*J. Phys. Chem. B* 2012, 116, 40–47

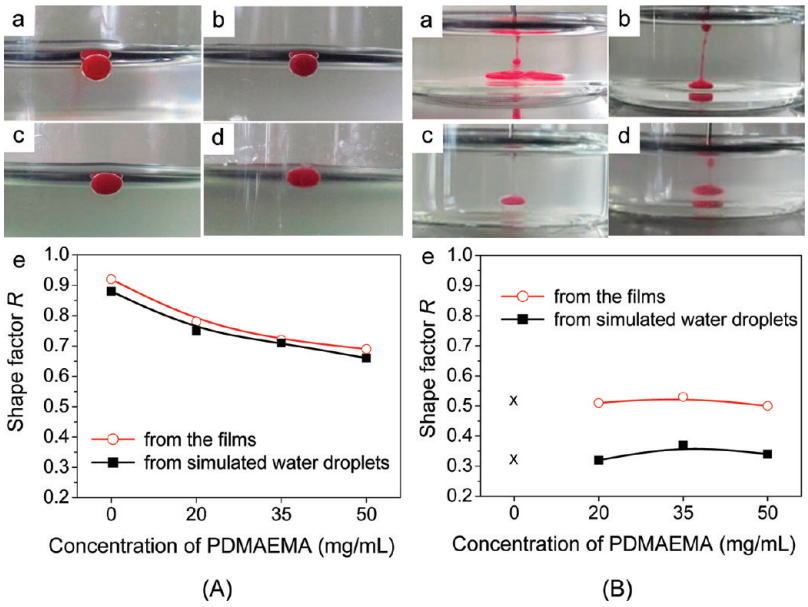

Figure 6. Simulated water droplets in solutions with different PDMAEMA concentrations: (a) 0 mg/mL; (b) 20 mg/mL; (c) 35 mg/mL; (d) 50 mg/mL. The concentration of PS is kept constant at 100 mg/mL. (e) Dependence of shape factor *R* on the concentration of PDMAEMA. Solvent: (A) CF and (B) THF.

Table 1. Surface Tension of the Solutions Measured by the Pendant Drop Method

	γ (mN/m)			γ (mN/m)
sample	CF	THF	sample	water
solvent	27.2	26.4	solvent	74.3
PS (20 mg/mL)	26.5	26.0	PDMAEMA (5 mg/mL)	65.9
PS/PDMAEMA (20/4 mg/mL)	26.9	25.7	PDMAEMA (10 mg/mL)	65.8
PS/PDMAEMA (20/7 mg/mL)	26.6	26.1	PDMAEMA (20 mg/mL)	65.3
PS/PDMAEMA (20/10 mg/mL)	26.2	25.4	PDMAEMA (50 mg/mL)	65.1
PS (100 mg/mL)	26.4	25.6		
PS/PDMAEMA (100/20 mg/mL)	26.5	24.9		
PS/PDMAEMA (100/35 mg/mL)	26.3	25.1		
PS/PDMAEMA (100/50 mg/mL)	26.1	25.0		

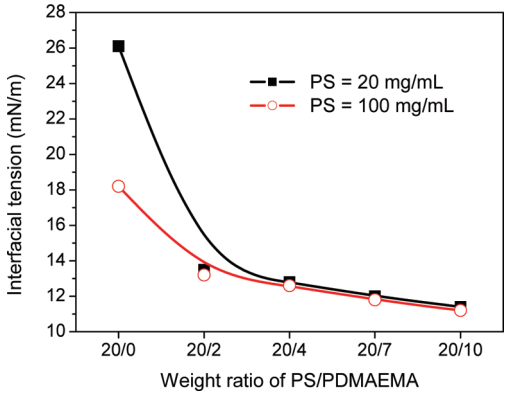

Figure 7. Interfacial tensions between water and PS/PDMAEMA solutions. The solvent is CF.

by the pendant drop technique,[35] and the results are summarized in Table 1. It is obvious that for either CF or THF, the surface tensions of the polymer solutions with different PS concentrations and different additive contents are almost the same with that of the solvent. Considering that the water-soluble additives such as PDMAEMA may diffuse into the water droplets because they are strongly hygroscopic,[38] the surface tensions of the PDMAEMA aqueous solutions were also measured. Results indicate that the surface tension of the PDMAEMA aqueous solution decreases slightly compared with that of deionized water. As a small amount of PDMAEMA is able to cover the surface of the water droplets, further increasing the content of PDMAEMA has a little influence on the surface intension.

The interfacial tensions between water and PS/PDMAEMA CF solutions are shown in Figure 7. We found that the interfacial tension decreases with the content of PDMAEMA, no matter if at initial concentration state (PS = 20 mg/mL) or highly concentrated state (PS = 100 mg/mL). Moreover, this decrease is larger (from 26 mN/m to ~12 mN/m) than that in the surface tensions. The decrease of interfacial tension may be caused by aggregation of the hydrophilic additive at the interface of water and the

dx.doi.org/10.1021/jp208115u |J. Phys. Chem. B 2012, 116, 40–47

Scheme 2. Schematic Illustration of the Water Droplet at the Air/Polymer Solution Interface

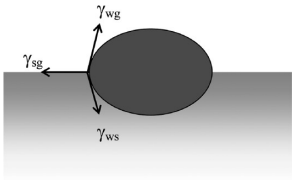

polymer solution. For the THF system, the interfacial tensions between water and the polymer solutions are difficult to credibly measure.

DISCUSSION

It is generally believed that during the breath figure process the condensed water droplets can be stabilized by the precipitation of polymers without polar groups such as linear and star PS or by the assembly of block copolymers, hydrophilic polymers, surfactants, nanogels, and nanoparticles.[2,3,38−43] For example, Gu et al. suggested that Ag nanoparticles can adsorb at the water/solvent interface and stabilize the interface, forming a mechanically resistant layer to prevent the water droplet from dissolving with the polymer solution.[39] In fact, the pores are shaped by the condensed and stabilized water droplets, which act as dynamic templates. In other words, the interfacial behaviors of the water droplets on/in the polymer solutions are crucial to the pore structures of the films when neglecting the influence of gravity of the water droplets or pressure induced by the solution. Using CF that is immiscible with water as the solvent, the water droplets float on/in the solution, and hence, the spreading behavior determines their shape. In the case of THF, the water droplets sink into the solution and can be dragged to the edge of the solution by convection flow and finally locate at an air/solution interface.[44] Therefore, the shape of the water droplets in THF solutions is also affected by the spreading behavior. The spreading coefficient S, the work done in spreading water droplets over a unit area of polymer solution surface, was defined as[45]

$$S = \gamma_{sg} - (\gamma_{wg} + \gamma_{ws}) \quad (1)$$

where γ_{sg} is the surface tension of polymer solution; γ_{wg} is the surface tension of water droplet; and γ_{ws} is the interfacial tension between the polymer solution and the water droplet in this case (Scheme 2). $S \geq 0$ means complete wetting and $S < 0$ indicates partial wetting. The water droplet maintains a spherical or near-spherical shape only at a small spreading coefficient value.

As mentioned above, the surface tensions of the polymer solutions change little (Table 1). Therefore, the term γ_{sg} in eq 1 almost keeps constant. Results also indicate that the term γ_{wg} decreases slightly when a hydrophilic additive such as PDMAEMA was introduced. Therefore, the spreading coefficient S of the water droplet in the blending system mainly depends on the interfacial tension between the water droplet and the polymer solution, i.e., γ_{ws}. It can be seen from Figure 7 that the interfacial tension decreases remarkably with the content of PDMAEMA. According to eq 1, the spreading coefficient S of the water droplet increases with the decrease of the interfacial tension. Therefore, it is reasonable that the water droplets in CF solutions change from near-spherical to ellipsoidal as increasing the PDMAEMA content (Figure 6A).

For the THF system, the additive is necessary for the formation of patterned films. When the THF solution of PS was employed in the breath figure method, there are no pores on the film surface because water is mixed with THF, which is confirmed by both the experimental (Figure 4a) and simulated (Figure 6B) results. Although the interfacial tensions between water and the THF solutions are speculated to be small or even zero,[39] they cannot be credibly measured. It should be also noted that once the drop is at the bottom, other effects also become important in determining its shape, for instance, the interfacial tension between the substrate and the water droplet. Small γ_{ws} induces a large spreading coefficient S and hence generates ellipsoidal pores. However, it is known that hydrophilic additives may diffuse into the water droplets, and the surface tentions of the PDMAEMA aqueous solutions change little with the content of PDMAEMA. Therefore, there is no obvious change in the shape factor R with the content of additives in the THF solutions.

It seems that the aggregation of additives at the interface plays an important role in the pore structure. This aggregation is followed by the precipitation of PS, which is less active at the interface. In the CF system, the additive aggregates around the water droplets and decreases the interfacial tension. The surface coverage of the water droplets increases with the additive concentration, and the pore shape change from near-spherical to ellipsoidal. In the THF system, the water droplets can be totally covered by the additive even at a low concentration. There is no obvious change in the pore shape with the increase of additive content in the THF solution. It can be deduced that the aggregation of additives in the THF system is more efficient than that in the CF system, which can be demonstrated by verifying the distribution of additives on the patterned films.

PS/PDMAEMA films prepared from the CF solution or the THF solution can be immersed in *p*-xylylene dichloride (XDC) solution for quaternization/cross-linking.[46] After cross-linking, the film prepared from the CF solution becomes disordered (see the Supporting Information). There is no obvious border between the PS phase and the cross-linked PDMAEMA phase, which indicates that PDMAEMA is not totally located at the interface (the pore wall). However, the film prepared from the THF solution shows an effective aggregation of PDMAEMA in the pores. The distribution of PDMAEMA on the films was further characterized by the adsorption of fluorescein sodium salt, which is a negatively charged dye and can be adsorbed on positively charged films. Therefore, it can be proved that the aggregation of PDMAEMA in the THF system is indeed more efficient than that in the CF system.

Finally, it should be noted that the water droplet could be covered with a thin film of solvent or solution in a breath figure process.[47] As a result, the water droplet only makes contact with the polymer solution and does not contact the air. However, according to above-mentioned results, the shape of water droplets is mainly determined by the interfacial tension between water and the polymer solution, instead of the air/water interface. Therefore, the existence of a water/air interface or not does not remarkably affect the conclusion.

CONCLUSIONS

Honeycomb-patterned films with controlled pore shape have been prepared from commercially available PS using water-soluble polymers, including PDMAEMA, PEG, and PVP, as the additives. The pores can be modulated between near-spherical and

ellipsoidal shape by changing the solvent and the additive content. Using CF as the solvent, the pores gradually change from near-spherical to ellipsoidal with the increase of additive content, which is mainly induced by the decrease of interfacial tension between water and the polymer solution. However, only ellipsoidal pores are formed from the THF solutions because the aggregation of a hydrophilic additive in the THF system is more efficient than that in the CF system, and the aggregated hydrophilic additive stabilizes the condensed water droplets, which shape the pores. This study facilitates our understanding of the dynamic breath figure process and provides a new pathway to control the shape, in addition to the size, of the breath figures.

■ ASSOCIATED CONTENT

Supporting Information. Micrographs of films prepared under different conditions and cross-linked samples. This material is available free of charge via the Internet at http://pubs.acs.org.

■ AUTHOR INFORMATION

Corresponding Author

*Fax: +86-571-87951592. E-mail: lswan@zju.edu.cn.

■ ACKNOWLEDGMENT

Financial support from the National Natural Science Foundation of China (51173161, 50803053), the Zhejiang Provincial Natural Science Foundation of China (Y4110076), the Program for Zhejiang Provincial Innovative Research Team (2009R50004), and Fundamental Research Funds for the Central Universities (MOE Engineering Research Center of Membrane and Water Treatment Technology) is gratefully acknowledged.

■ REFERENCES

(1) Widawski, G.; Rawieso, M.; Francois, B. *Nature* **1994**, *369*, 387–389.
(2) Bunz, U. H. F. *Adv. Mater.* **2006**, *18*, 973–986.
(3) Stenzel, M. H.; Barner-Kowollik, C.; Davis, T. P. *J. Polym. Sci. Part A: Polym. Chem.* **2006**, *44*, 2363–2375.
(4) Tsai, H. H.; Xu, Z. H.; Pai, R. K.; Wang, L. Y.; Dattelbaum, A. M.; Shreve, A. P.; Wang, H. L.; Cotlet, M. *Chem. Mater.* **2011**, *23*, 759–761.
(5) Yin, S. Y.; Zhang, Y. Y.; Kong, J. H.; Zou, C. J.; Li, C. M.; Lu, X. H.; Ma, J.; Boey, F. Y. C.; Chen, X. D. *ACS Nano* **2011**, *5*, 3831–3838.
(6) Kon, K.; Brauer, C. N.; Hidaka, K.; Lohmannsroben, H. G.; Karthaus, O. *Langmuir* **2010**, *26*, 12173–12176.
(7) Zander, N. E.; Orticki, J. A.; Karikari, A. S.; Long, T. E.; Rawlett, A. M. *Chem. Mater.* **2007**, *19*, 6145–6149.
(8) Zhu, Y.; Sheng, R.; Luo, T.; Li, H.; Sun, J.; Chen, S.; Sun, W.; Cao, A. M. *ACS Appl. Mater. Interfaces* **2011**, *3*, 2487–2495.
(9) Ishii, D.; Yabu, H.; Shimomura, M. *Chem. Mater.* **2009**, *21*, 1799–1801.
(10) Stenzel-Rosenbaum, M. H.; Davis, T. P.; Fane, A. G.; Chen, V. *Angew. Chem., Int. Ed.* **2001**, *40*, 3428–3432.
(11) Ke, B. B.; Wan, L. S.; Zhang, W. X.; Xu, Z. K. *Polymer* **2010**, *51*, 2168–2176.
(12) Yabu, H.; Tanaka, M.; Ijiro, K.; Shimomura, M. *Langmuir* **2003**, *19*, 6297–6300.
(13) Wang, L. H.; Tian, Y.; Ding, H. Y.; Liu, B. Q. *Eur. Polym. J.* **2007**, *43*, 862–869.
(14) Kabuto, T.; Hashimoto, Y.; Karthaus, O. *Adv. Funct. Mater.* **2007**, *17*, 3569–3573.
(15) Tang, P. Q.; Hao, J. C. *J. Colloid Interface Sci.* **2009**, *333*, 1–5.
(16) Connal, L. A.; Vestberg, R.; Hawker, C. J.; Qiao, G. G. *Adv. Funct. Mater.* **2008**, *18*, 3315–3322.
(17) Peng, J.; Han, Y. C.; Yang, Y. M.; Li, B. Y. *Polymer* **2004**, *45*, 447–452.
(18) Cui, L.; Xuan, Y.; Li, X.; Ding, Y.; Li, B. Y.; Han, Y. C. *Langmuir* **2005**, *21*, 11696–11703.
(19) Kim, J. K.; Taki, K.; Ohshima, M. *Langmuir* **2007**, *23*, 12397–12405.
(20) Fukuhira, Y.; Yabu, H.; Ijiro, K.; Shimomura, M. *Soft Matter* **2009**, *5*, 2037–2041.
(21) Sun, H.; Li, H. L.; Wu, L. X. *Polymer* **2009**, *50*, 2113–2122.
(22) Dong, W. Y.; Zhou, Y. F.; Yan, D. Y.; Mai, Y. Y.; He, L.; Jin, C. Y. *Langmuir* **2009**, *25*, 173–178.
(23) Ke, B. B.; Wan, L. S.; Xu, Z. K. *Langmuir* **2010**, *26*, 8946–8952.
(24) Ke, B. B.; Wan, L. S.; Chen, P. C.; Zhang, L. Y.; Xu, Z. K. *Langmuir* **2010**, *26*, 15982–15988.
(25) Connal, L. A.; Qiao, G. G. *Adv. Mater.* **2006**, *18*, 3024–3028.
(26) Park, J. S.; Lee, S. H.; Han, T. H.; Kim, S. O. *Adv. Funct. Mater.* **2007**, *17*, 2315–2320.
(27) Li, L.; Zhong, Y. W.; Gong, J. L.; Li, J. A.; Chen, C. K.; Zeng, B. R.; Ma, Z. *Soft Matter* **2011**, *7*, 546–552.
(28) Jiang, X. L.; Zhang, T. Z.; Xu, L. N.; Wang, C. L.; Zhou, X. F.; Gu, N. *Langmuir* **2011**, *27*, 5410–5419.
(29) Nishikawa, T.; Nonomura, M.; Arai, K.; Hayashi, J.; Sawadaishi, T.; Nishiura, Y.; Hara, M.; Shimomura, M. *Langmuir* **2003**, *19*, 6193–6201.
(30) Yabu, H.; Shimomura, M. *Langmuir* **2005**, *21*, 1709–1711.
(31) Chen, P. C.; Wan, L. S.; Ke, B. B.; Xu, Z. K. *Langmuir* **2011**, *27*, 12597–12605.
(32) Yabu, H.; Jia, R.; Matsuo, Y.; Ijiro, K.; Yamamoto, S.; Nishino, F.; Takaki, T.; Kuwahara, M.; Shimomura, M. *Adv. Mater.* **2008**, *20*, 4200–4207.
(33) Connal, L. A.; Vestberg, R.; Hawker, C. J.; Qiao, G. G. *Adv. Funct. Mater.* **2008**, *18*, 3706–3714.
(34) Ke, B. B.; Wan, L. S.; Li, Y.; Xu, M. Y.; Xu, Z. K. *Phys. Chem. Chem. Phys.* **2011**, *13*, 4881–4887.
(35) Anderson, K. E.; Rogers, J. A.; Li, D. Q. *J. Pharm. Pharmacol.* **1997**, *49*, 587–591.
(36) Srinivasarao, M.; Collings, D.; Philips, A.; Patel, S. *Science* **2001**, *292*, 79–83.
(37) Bolognesi, A.; Mercogliano, C.; Yunus, S.; Civardi, M.; Comoretto, D.; Turturro, A. *Langmuir* **2005**, *21*, 3480–3485.
(38) Cui, L.; Han, Y. C. *Langmuir* **2005**, *21*, 11085–11091.
(39) Jiang, X. L.; Zhou, X. F.; Zhang, Y.; Zhang, T. Z.; Guo, Z. R.; Gu, N. *Langmuir* **2010**, *26*, 2477–2483.
(40) Sun, W.; Ji, J.; Shen, J. C. *Langmuir* **2008**, *24*, 11338–11341.
(41) Sun, H.; Li, W.; Wu, L. X. *Langmuir* **2009**, *25*, 10466–10472.
(42) Ma, H. M.; Hao, J. C. *Chem.—Eur. J.* **2010**, *16*, 655–660.
(43) Poly, J.; Ibarboure, E.; Le Meins, J.-F.; Rodriguez-Hernandez, J.; Taton, D.; Papon, E. *Langmuir* **2011**, *27*, 4290–4295.
(44) Maruyama, N.; Koito, T.; Nishida, J.; Sawadaishi, T.; Cieren, X.; Ijiro, K.; Karthaus, O.; Shimomura, M. *Thin Solid Films* **1998**, *327*, 854–856.
(45) Dobbs, H.; Bonn, D. *Langmuir* **2001**, *17*, 4674–4676.
(46) Yang, Y. F.; Wan, L. S.; Xu, Z. K. *J. Membr. Sci.* **2009**, *337*, 70–80.
(47) Bormashenko, E.; Bormashenko, Y.; Whyman, G.; Pogreb, R.; Gendelman, O. *Macromol. Chem. Phys.* **2007**, *208*, 702–709.